J Appl Physiol 138: 342–357, 2025.
First published November 26, 2024; doi:10.1152/japplphysiol.00357.2024

american physiological society

JOURNAL OF APPLIED PHYSIOLOGY

RESEARCH ARTICLE

N_2 exchanges in hyperbaric environments: toward a model based on physiological gas transport (O_2 and CO_2)

Michael Theron,[1] Alexis Blasselle,[2] Lisa Nedellec,[1] Pascal Ballet,[3] Emmanuel Dugrenot,[1,2,4,5] Bernard Gardette,[2] François Guerrero,[1] Anne Henckes,[6] and Jean-Pierre Pennec[1]

[1]*ORPHY Laboratory, Université de Brest, Brest, France;* [2]*Tek Diving SAS, Brest, France;* [3]*LaTIM (Laboratoire de Traitement de l'Information Médicale), UMR 1101, Université de Brest, Brest, France;* [4]*Divers Alert Network, Durham, North Carolina, United States;* [5]*Joint Department of Biomedical Engineering, The University of North Carolina and North Carolina State University, Chapel Hill, North Carolina, United States; and* [6]*Unité de Médecine Hyperbare CHRU, Brest, France*

Abstract

Decompression sickness can occur in divers even when recommended decompression procedures are followed. Furthermore, the physiological state of individuals can significantly affect bubbling variability. These informations highlight the need for personalized input to improve decompression in SCUBA diving. The main objective of this study is to propose a fundamental framework for a new approach to inert gas exchanges. A physiological model of oxygen delivery to organs and tissues has been built and adapted to nitrogen. The validation of the model was made by transferring the N_2 to CO_2. Under normobaric conditions (air breathing, oxygen breathing, and static apnea) and hyperbaric conditions, the O_2 model replicates the reference physiological Po_2 (Spearman correlation tests $P < 0.001$). The inert gas models can simulate inert gas partial pressures under normobaric and hyperbaric conditions. However, the lack of reference values prevents direct validation of this new model. Therefore, the N_2 model has been transferred to CO_2. The resulting CO_2 model has been validated by comparing it with physiological reference values (Spearman correlation tests $P < 0.01$). The validity of the CO_2 model constructed from the N_2 model demonstrates the plausibility of this physiological model of inert gas exchanges. In the context of personalized decompression procedures, the proposed model is of significant interest as it enables the integration of physiological and morphological parameters (blood and respiratory flows, alveolo-capillary diffusion, respiratory and blood volumes, oxygen consumption rate, fat mass, etc.) into a model of nitrogen saturation/desaturation, in which oxygen and CO_2 partial pressures can also be incorporated.

NEW & NOTEWORTHY This is the first model of inert gas transport based on the physiology of respiratory gas. It was built for O_2 delivery and validated against literature data; it was then transposed to N_2 exchanges. The transposition procedure was checked by transposing the N_2 model to CO_2 (and validated against literature data). This model opens the possibility to integrate physiological and morphological inputs in a personalized decompression procedure in SCUBA diving.

decompression sickness; nitrogen; personalized decompression; physiological model; SCUBA diving

INTRODUCTION

SCUBA diving is a globally practiced recreational activity, and it serves various professional and recreative purposes such as aiding civil engineering, military operations, scientific research, and entertainment. The diverse demographic of diverse spans from physically fit youths to elderly individuals with varying health conditions. The spectrum of diving practices encompasses brief, shallow air dives to deep, protracted dives with the use of synthetic gas mixtures. Despite significant advances in decompression procedures, notably the transition from decompression tables to diving computers, incidents of decompression sickness (DCS) still occur.

Epidemiological data collected by the Divers Alert Network (DAN) has revealed instances of DCS occurrence in divers who adhere to their dive computer recommendations (1). In addition, long-term adverse effects have been documented in divers who have no history of diagnosed DCS (2). Furthermore, it has been observed that the incidence of "undeserved" DCS remains consistent regardless of the algorithm used for decompression (3). In the context of diving, preconditioning encompasses procedures implemented before a dive that can either enhance resistance to decompression stress or mitigate its severity (4). Studies on preconditioning strategies have shown that, for a given diver and dive profile, bubble formation can be significantly altered by influencing the physiological condition of individuals (5). Moreover, a recent study has discussed the potential involvement of physiological parameters in bubble formation variability (6). Cumulatively, these investigations underscore the necessity for personalized physiological input to enhance decompression models (Table 1).

Correspondence: M. Theron (Michael.theron@univ-brest.fr).
Submitted 14 May 2024 / Revised 29 October 2024 / Accepted 14 November 2024

Table 1. *Physiological inputs in the model and their reference values*

Physiological Parameter	Model Parameter	Reference Value	Bibliography
Ventilatory flow	$\dot{V}$	8.1 L·min^{-1}	(21, 22)
Mean expiratory reserve volume	V_{Aw}	1 L	(22)
Mean functional residual volume	V_{Alg}	1.5 L	(22)
Hb concentration	[Hb]	2.19 mmol·L^{-1}	(23)
Hb O_2 carrying capacity	Oxc	1.34 mL·g^{-1}	(24)
O_2 solubility in plasma	α_{O_2p}	9.97.10^{-6} mmol·L^{-1}·Pa^{-1}	(25)
N_2 solubility in plasma	α_{N_2p}	6.19.10^{-5} mmol·L^{-1}·Pa^{-1}	(26)
CO_2 solubility in plasma	α_{CO_2p}	2.25.10^{-4} mmol·L^{-1}·Pa^{-1}	(27)
Alveolar blood volume	V_{Alb}	0.5 L	(28)
Cardiac output	$\dot{Q}$	4.2 L·min^{-1}	(28)
Arterial blood volume	V_a	1.7 L	(28)
Capillary blood volume	V_c	0.5 L	(28)
Venous blood volume	V_V	3 L	(28)
Tissue volume	V_{ti}	70 L	
Metabolism	$\dot{M}O_2$	0.119 mmol·min^{-1}·kg^{-1}	(28)

Against this backdrop, the primary objective of this study is to lay the groundwork for a novel approach to inert gas exchanges in divers. Remarkably, despite more than a century of research in this field [since the inception of Haldane's model (7)], no decompression model has been based on the integrated physiology of gas delivery to tissues (8). On one hand, there exists highly complex mechanistic models designed to replicate respiratory and/or inert gas exchanges (9–11). Although these models excel at finely delineating pathophysiological conditions and gas exchange during anesthesia, their complexity far surpasses the requirements for decompression procedures, rendering their integration into dive computers challenging. Conversely, Haldanian or Bühlmann's models consider different compartments without establishing a direct connection to biological systems (12–14). The diffusive models from Hempleman (15) or Hills (16) aim at reproducing a single organ (an articulation). Bubble models developed by Hennessy (17), Chappell and Payne (18), or Hugon (19) encompass various tissues and organs on a physiological basis. However, in all these instances, the dynamics of inert gas transfer are predicated on relevant biophysical observations and hypotheses concerning diffusive and convective capacities, but not on the physiological dynamics of respiratory gas exchanges within the human body prohibiting the prediction of inert gas but also of O_2 and CO_2 exchange dynamics at the diver's scale.

In this context, we propose to base a new model of gas transfer on a well known gas: the O_2. In a first step, a physiological model of the O_2 delivery to organs and tissues is built. The results of this O_2 model are compared with reference physiological values and literature. In a second step, considering the differences of gas transportation and utilization, we transpose this model to inert gas exchanges. Nevertheless, due to the lack of experimental data, the N_2 model cannot be directly validated, hence, in a third step, the N_2 model is transposed to a CO_2 model that can be validated against reference values.

MATERIALS AND METHODS

Oxygen Model Structure and Equations

In its simplest structure (see Fig. 1), the model of oxygen transfer is composed of eight compartments:

- three gaseous one
  - inspired air
  - airways
  - alveolar gas
- four blood compartments
  - alveolar blood
  - arterial blood

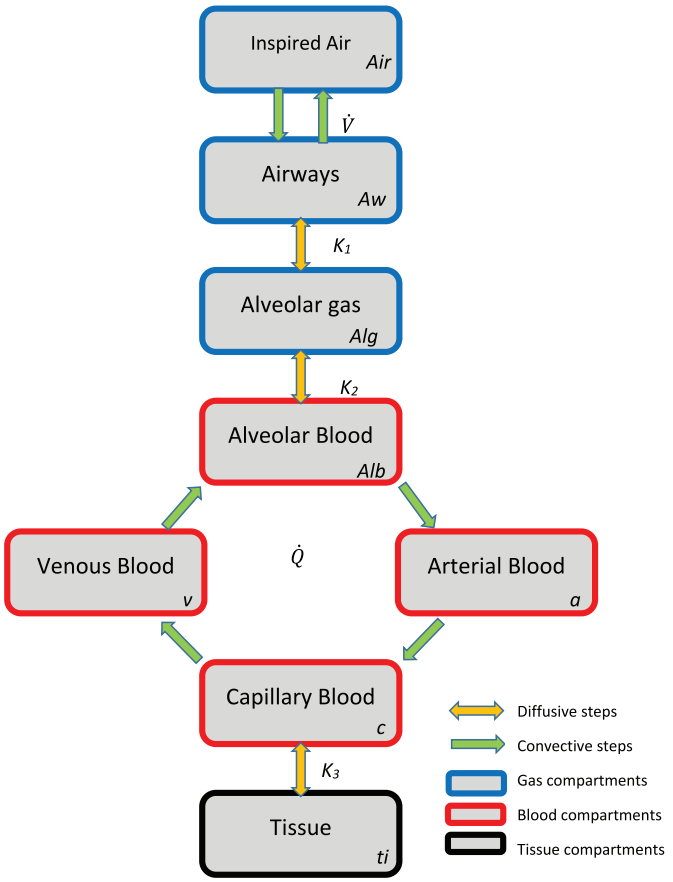

Figure 1. Model structure. a, arterial compartment; Alb, alveolar blood compartment; Alg, alveolar gas compartment; Aw, airways compartment; c, capillary blood compartment; K_1, K_2, K_3, diffusion coefficient of a gas at the interface between 1/the airways and the alveolar gas, 2/the alveolar gas and the alveolar blood, 3/the capillary blood and the corresponding tissue respectively; $\dot{Q}$, cardiac blood flow; ti, tissue compartment; v, venous compartment; $\dot{V}$, ventilatory flow.

  - capillaries blood
  - venous blood
- one tissue compartment.

The number of capillary beds and corresponding tissue compartments can be increased as needed to consider the diversity of organs. This point will be addressed in another work aiming at applying this model to the prevention of DCS.

Exchanges of O_2 between ambient air and airways on one hand and between the four blood compartments on the other hand are due to convective phenomenon (ventilatory and cardiac pumps). Exchanges at the interfaces

- airways/alveolar gas
- alveolar gas/alveolar blood
- capillary blood/tissue

are due to diffusive phenomena.

Gaseous Compartments

In the inspired air, the oxygen partial pressure is calculated from the ambient pressure (AP), the water vapor partial pressure at 37°C (P_{H_2O}), and the fraction of O_2 in the inspired gas (fr_{O_2}).

$$P_{O_2Air} = fr_{O_2}(AP - P_{H_2O}) \quad (1)$$

Considering hyperbaric environments, AP is a known function of time: AP = f(t).

The following assumptions are made:

- All the compartments' volumes are constant over time, hence their derivatives with respect to t are always equal to 0 (*NB*: it is possible to assume that the time derivative of the volume is known, leading to a general case exposed in the Supplemental calculations S1).
- All the gaseous phases obey Clausius-Clapeyron's ideal gas law, namely, PV = nRT.

In the other gaseous compartments, the oxygen partial pressure (Po_2) can be linked to the O_2 concentration (C) using the ideal gas law.

In the airways, the ideal gas law writes:

$$P_{O_2AW} = \frac{n_{O_2AW}}{V_{Aw}}RT = C_{O_2AW}RT$$

And in the alveolar gas:

$$P_{O_2Alg} = \frac{n_{O_2Alg}}{V_{Alg}}RT = C_{O_2Alg}RT$$

with V_{Aw} and V_{Alg}: mean volumes of gas in the airways and in the alveolar gas, R: ideal gas constant, and T: absolute temperature.

The variation of oxygen content in the airways (dn/dt) depends on the ventilatory convection from ambient air and diffusion to the alveolar compartment as follows:

$$\frac{dn_{O_2Aw}}{dt} = \dot{V}(C_{O_2Air} - C_{O_2Aw}) - K_{1O_2}(P_{O_2Aw} - P_{O_2Alg})$$

where $\dot{V}$ is the ventilatory flow, K_{1O_2} is the diffusion coefficient between the airways and the alveolar gas, C_{O_2Air} is the O_2 concentration in ambient air, C_{O_2Aw} and P_{O_2Aw} are the O_2 concentration and partial pressure in the airways, and P_{O_2Alg} is the O_2 partial pressure in the alveolar gas.

Considering the ideal gas law, the previous equation leads to:

$$\frac{dP_{O_2Aw}}{dt} = \frac{\dot{V}(C_{O_2Air} - C_{O_2Aw})RT}{V_{Aw}} - \frac{K_{1O_2}(P_{O_2Aw} - P_{O_2Alg})RT}{V_{Aw}}$$

and

$$\frac{dP_{O_2Aw}}{dt} = \frac{\dot{V}(P_{O_2Air} - P_{O_2Aw}) - K_{1O_2}(P_{O_2Aw} - P_{O_2Alg})RT}{V_{Aw}}$$

which can be rewritten:

$$\frac{dP_{O_2Aw}}{dt} = \frac{\dot{V}}{V_{Aw}}P_{O_2Air} - \frac{\dot{V} + K_{1O_2}RT}{V_{Aw}}P_{O_2Aw} + \frac{K_{1O_2}RT}{V_{Aw}}P_{O_2Alg} \quad (1_{O_2})$$

In a similar way, in the alveolar gas compartment (Alg), the variation of oxygen content can be described as the result of diffusion from alveolar gas to alveolar blood (alveolo-capillary diffusion):

$$\frac{dn_{O_2Alg}}{dt} = K_{1O_2}(P_{O_2Aw} - P_{O_2Alg}) - K_{2O_2}(P_{O_2Alg} - P_{O_2Alb})$$

in which K_{2O_2} is the diffusion coefficient between the alveolar gas and the alveolar blood and P_{O_2Alb} is the oxygen partial pressure in the alveolar blood.

From this equation, it is possible to write:

$$\frac{dP_{O_2Alg}}{dt} = \frac{[K_{1O_2}(P_{O_2Aw} - P_{O_2Alg}) - K_{2O_2}(P_{O_2Alg} - P_{O_2Alb})]RT}{V_{Alg}}$$

which can be rewritten as well:

$$\frac{dP_{O_2Alg}}{dt} = -\frac{RT}{V_{Alg}}(K_{2O_2} + K_{1O_2})P_{O_2Alg} + \frac{RT}{V_{Alg}}[K_{1O_2}P_{O_2Aw} + K_{2O_2}P_{O_2Alb}] \quad (2_{O_2})$$

with V_{Alg}: mean alveolar gas volume.

Blood Compartments

In the blood compartments, the O_2 concentration depends on the O_2 partial pressure through the dissolved O_2 fraction and the fraction of O_2 linked to the hemoglobin (noted Hb in what follows).

The dissolved O_2 concentration (C_{dO_2}) can be computed from Henry's law, knowing the oxygen solubility constant in the plasma (α_{O_2p}) and the oxygen partial pressure:

$$C_{dO_2} = \alpha_{O_2p}P_{O_2}$$

The concentration of O_2 carried on hemoglobin (C_{O_2Hb}) can be calculated from the Hb saturation (Sat), the O_2 carrying capacity of the Hb (Oxc), and the Hb concentration ([Hb]):

$$C_{O_2Hb} = Sat[Hb]Oxc$$

The hemoglobin saturation obeys Hill's equation (20):

$$Sat = \left[\left(a\left(P_{O_2}^3 + bP_{O_2}\right)^{-1}\right) + 1\right]^{-1}$$

in which

- $a = 2.34 \times 10^4$ and $b = 1.5 \times 10^2$ if P_{O_2} is expressed in Torr and
- $a = 5.5 \times 10^{10}$ and $b = 2.5 \times 10^6$ if P_{O_2} is expressed in Pa.

Hence, the total O_2 concentration (C_{O_2}) is a function of the oxygen partial pressure, noted $f(P_{O_2})$ (see Supplemental calculations S1 for the study of the function *f*):

$$C_{O_2} = f(P_{O_2}) = \left[\left(a\left(P_{O_2}^3 + bP_{O_2}\right)^{-1}\right) + 1\right]^{-1}[Hb]Oxc + {}_{\alpha O_2 p}P_{O_2}$$

Considering that in a given compartment i, $Q_{O_2 i} = V_i C_{O_2 i}$, and our assumption on the constant volumes over time, it is possible to express the derivative of $Q_{O_2 i}$ as:

$$\frac{dn_{O_2 i}}{dt} = Vi\frac{dP_{O_2 i}}{dt}f'(P_{O_2 i}) \qquad (\alpha)$$

where

$$f'(P_{O_2 i}) = \frac{a[Hb]Oxc(3P_{O_2 i}^2 + b)}{(P_{O_2 i}^3 + bP_{O_2 i} + a)^2} + \alpha_{O_2 p}$$

The variation of oxygen content in the alveolar blood depends on:

1) on the alveolo-capillary diffusion from alveolar gas,
2) on the oxygen flow to the arterial compartment and
3) on the oxygen flow from the venous compartment:

$$\frac{dn_{O_2 Alb}}{dt} = K_{2O_2}\left(P_{O_2 Alg} - P_{O_2 Alb}\right) - \dot{Q}C_{O_2 Alb} + \dot{Q}C_{O_2 v}$$

(with $\dot{Q}$: cardiac blood flow).
That can be written:

$$\frac{dn_{O_2 Alb}}{dt} = K_{2O_2}\left(P_{O_2 Alg} - P_{O_2 Alb}\right) + \dot{Q}(C_{O_2 v} - C_{O_2 Alb})$$

Hence, considering *Eq.* α:

$$\frac{dP_{O_2 Alb}}{dt} = \frac{1}{V_{Alb} * f'(P_{O_2 Alb})}\left[K_{2O_2}\left(P_{O_2 Alg} - P_{O_2 Alb}\right)\right.$$

$$\left. + \dot{Q}\left(f(P_{O_2 v}) - f(P_{O_2 Alb})\right)\right] \qquad (3_{O_2})$$

As there is no direct diffusion of oxygen from the arterial compartment to the surrounding tissues, the variation of oxygen content depends only on *1*) the inlets from alveolar blood and *2*) the outlets to the capillaries:

$$\frac{dn_{O_2 a}}{dt} = \dot{Q}C_{O_2 Alb} - \dot{Q}C_{O_2 a}$$

Consequently:

$$\frac{dn_{O_2 a}}{dt} = \dot{Q}(C_{O_2 Alb} - C_{O_2 a})$$

And similarly:

$$\frac{dP_{O_2 a}}{dt} = \frac{\dot{Q}}{V_a f'(P_{O_2 a})}\left[f(P_{O_2 Alb}) - f(P_{O_2 a})\right] \qquad (4_{O_2})$$

In the capillaries, the situation is close to the one in the alveolar blood compartment: the variations of O_2 content are due to one diffusive step (to the tissue) and two convective steps (from arteries and to the venous compartment):

$$\frac{dn_{O_2 c}}{dt} = \dot{Q}(C_{O_2 a} - C_{O_2 c}) - K_{3O_2}(P_{O_2 c} - P_{O_2 ti})$$

in which K_3 is the diffusion coefficient between the capillary blood and the corresponding tissue.

Hence:

$$\frac{dP_{O_2 c}}{dt} = \frac{1}{V_c f'(P_{O_2 c})}\left[\dot{Q}(f(P_{O_2 a}) - f(P_{O_2 c})) - K_{3O_2}(P_{O_2 c} - P_{O_2 ti})\right] \qquad (5_{O_2})$$

At last, the venous situation is equivalent to the arterial one:

$$\frac{dn_{O_2 v}}{dt} = \dot{Q}(C_{O_2 c} - C_{O_2 v})$$

And:

$$\frac{dP_{O_2 v}}{dt} = \frac{\dot{Q}}{V_v f'(P_{O_2 v})}\left[f(P_{O_2 c}) - f(P_{O_2 v})\right] \qquad (6_{O_2})$$

Tissue Compartments

Regarding the calculation of the O_2 partial pressure in the tissue compartment, the situation is simpler than in the blood compartment, as the O_2 is only present in a dissolved state:

$$P_{O_2 ti} = \frac{C_{O_2 ti}}{\alpha_{O_2 ti}}$$

The variations of O_2 content in this compartment are the consequences of the income from the capillary bed and the oxygen consumption from the metabolism:

$$\frac{dn_{O_2 ti}}{dt} = K_{3O_2}(P_{O_2 c} - P_{O_2 ti}) - \dot{M}O_2$$

And, as there is no hemoglobin in tissues, $f' = \alpha_{O_2 ti}$
Hence:

$$\frac{dP_{O_2 ti}}{dt} = \frac{1}{V_t \alpha_{O_2 ti}}\left[K_{3O_2}(P_{O_2 c} - P_{O_2 ti}) - \dot{M}O_2\right] \qquad (7_{O_2})$$

It is possible to increase the number of tissue compartments considering an equal number of capillaries compartments. For each tissue compartment tiα, there is a capillary compartment cα in which:

$$\frac{dn_{O_2 c\alpha}}{dt} = \dot{Q}\alpha(f(P_{O_2 a}) - f(P_{O_2 c\alpha})) - K_{3\alpha O_2}(P_{O_2 c\alpha} - P_{O_2 ti\alpha})$$

and

$$\frac{dn_{O_2 ti\alpha}}{dt} = K_{3\alpha O_2}(P_{O_2 c\alpha} - P_{O_2 ti\alpha}) - \dot{M}O_{2\alpha}$$

which can be written:

$$\frac{dP_{O_2 ti\alpha}}{dt} = \frac{1}{V_{ti\alpha}\alpha_{O_2 ti\alpha}}\left[K_{3\alpha O_2}(P_{O_2 c\alpha} - P_{O_2 ti\alpha}) - \dot{M}O_{2\alpha}\right]$$

In this system,

$$\sum_{1\to n}\dot{Q}_\alpha = \dot{Q} \quad \text{and} \quad \sum_{1\to n}\dot{M}O_\alpha = \dot{M}O_2$$

$P_{O_2 c\alpha}$ and $P_{O_2 ti\alpha}$ are the O_2 partial pressures in the capillaries and in the tissues α, V_{ca}, and V_{tia} the volumes of these compartments, $K_{3\alpha O_2}$ is the diffusion coefficient between the capillary bed and the tissue of interest, $\alpha_{O_2 ti\alpha}$ the O_2 solubility coefficient in tiα, Q_a the blood flow in the capillary bed and $\dot{M}O_{2\alpha}$ the O_2 consumption in this tissue.

Table 2. *Oxygen partial pressures reference values by compartments (breathing air at atmospheric pressure)*

Compartments	Model Parameter	P_{O_2} Reference Values mmHg	P_{O_2} Reference Values kPa
Airways	P_{AW}	120–130	16.0–17.3
Alveolar gas	P_{Alg}	100–110	13.3–14.7
Arterial blood	P_a	90–98	12.0–13.1
Venous blood	P_v	40–50	5.3–6.7
Tissues	P_{ti}	5–20	0.7–2.7

Oxygen Model Parameters

From *Eqs. 1–7*, and under the assumption that all the volumes are constant over time, a differential system can be established, whose numerical resolution gives access to the oxygen partial pressures over time in any compartment.

Inputs.
The external input of the system is the inspired oxygen partial pressure (P_{O_2Air}), which is a function of the ambient pressure (AP) and the oxygen fraction (fr_{O_2}) (see *Eq. α*).

The different equations of the model are based on a set of physiological parameters summarized in the Table 1. In the present paper, these parameters are considered as constants and are given with their corresponding reference values (N.B.: Some of them could also be considered as variables and used as inputs in a model considering cardiorespiratory and metabolic modifications during a dive).

Outputs.
The outputs of the model are the oxygen partial pressures in the different compartments. Table 2 recapitulates these parameters given with their reference values for O_2 (breathing air at atmospheric pressure).

Diffusion coefficients.
In the set of *Eqs. 1–7*, the various diffusion coefficients are the following:

- K_{1O_2} for the diffusion from the airways to the alveolar gas,
- K_{2O_2} for the diffusion from the alveolo-capillary part to the capillary,
- K_{3O_2} for the tissue diffusion.

Considering a steady state (i.e., $\frac{dP}{dt} = 0$), these coefficients can be determined respectively from *Eqs. 1*, *2*, and *7*:

$$K_{1O_2} = \frac{\dot{V}(P_{O_2Air} - P_{O_2Aw})}{(P_{O_2Aw} - P_{O_2Alg})RT}$$

$$K_{2O_2} = \frac{K_{1O_2}(P_{O_2Aw} - P_{O_2Alg})}{(P_{O_2Alg} - P_{O_2Alb})}$$

$$K_{3O_2} = \frac{\dot{M}O_2}{(P_{O_2c} - P_{O_2ti})}$$

The numerical values obtained from this equation set (and from the values indicated in Tables 1 and 2) for the three diffusion coefficients are given in Table 3.

Model Transposition from O_2 to N_2

Once established for O_2 transport, the set of differential *Eqs. 1–7* can be adapted to inert gases, for instance N_2. In fact, this transposition simplifies the equation set since:

1) those gases are only present in a dissolved form and the problem of hemoglobin transport does not exist anymore,
2) there is no inert gases metabolism and they will only accumulate in tissues, or vanish from them.

Consequently, the set of equations defining N_2 gas transport can be written as follow:

$$\frac{dP_{N_2Aw}}{dt} = \frac{\dot{V}}{V_{Aw}}P_{N_2Air} - \frac{\dot{V} + K_{1N_2}RT}{V_{Aw}}P_{N_2Aw} + \frac{K_{1N_2}RT}{V_{Aw}}P_{N_2Alg} \qquad (1_{N_2})$$

$$\frac{dP_{N_2Alg}}{dt} = -\frac{RT}{V_{Alg}}(K_{1N_2} + K_{2N_2})P_{N_2Alg} + \frac{RT}{V_{Alg}}\left[K_{1N_2}P_{N_2Aw} + K_{2N_2}P_{N_2Alb}\right] \qquad (2_{N_2})$$

$$\frac{dP_{N_2Alb}}{dt} = \frac{1}{\alpha_{N_2}V_{Alb}}\left[K_{2N_2}P_{N_2Alg} - P_{N_2Alb}\left(K_{2N_2} + \alpha_{N_2}\dot{Q}\right) + \alpha_{N_2}\dot{Q}P_{N_2v}\right] \qquad (3_{N_2})$$

$$\frac{dP_{N_2a}}{dt} = \frac{\dot{Q}}{V_a}(P_{N_2Alb} - P_{N_2a}) \qquad (4_{N_2})$$

$$\frac{dP_{N_2c}}{dt} = \frac{1}{\alpha_{N_2}V_c}\left[\alpha_{N_2}\dot{Q}P_{N_2a} - \left(\alpha_{N_2}\dot{Q} + K_{3N_2}\right)P_{N_2c} + K_{3N_2}P_{N_2ti}\right] \qquad (5_{N_2})$$

$$\frac{dP_{N_2v}}{dt} = \frac{\dot{Q}}{V_v}(P_{N_2c} - P_{N_2v}) \qquad (6_{N_2})$$

$$\frac{dP_{N_2ti}}{dt} = \frac{K_{3N_2}}{\alpha_{N_2ti}V_{ti}}(P_{N_2c} - P_{N_2ti}) \qquad (7_{N_2})$$

Table 3. *Diffusion coefficients determination*

Diffusion Interface	Model Parameter	Diffusion Coefficients (in $mmol \cdot min^{-1} \cdot Pa^{-1}$) O_2 Range of Calculated Values	O_2 Values Used in the Model	N_2 Values Used in the Model	CO_2 Values Used in the Model
Airways – alveolar gas	K_1	2.0×10^{-3}–6.9×10^{-3}	2.50×10^{-3}	2.67×10^{-3}	2.13×10^{-3}
Alveolar gas – alveolar blood	K_2	4.6×10^{-3}–2.7×10^{-2}	7.00×10^{-3}	7.48×10^{-3}	5.97×10^{-3}
Capillary bed – Tissue	K_3	1.6×10^{-3}–1.2×10^{-2}	2.50×10^{-3}	2.67×10^{-3}	2.13×10^{-3}

Table 4. *Coefficients of the equation* $pH = h(Pco_2)$

C_0	7.6897094
C_1	0.49083576
C_2	−0.098342987
C_3	0.0053348381
C_4	−0.00011621357

These coefficients have been established with the software *SciDAVis*.

In the case of O_2 transport, the diffusion coefficients K_{1O_2}, K_{2O_2}, and K_{3O_2} can be determined, as the O_2 cascade is completely known. The same approach cannot be applied in the case of inert gases.

In the present model, coefficients K_{1N_2}, K_{2N_2}, and K_{3N_2} are defined using the Graham's law that states that the diffusion coefficient of a given species is inversely proportional to the square root of its molecular weight (Mw). Applied to the present problem, this law enables to compare the diffusion coefficients of the O_2 to the ones of another gas (19). This can be expressed as:

$$\frac{K_{N_2}}{K_{O_2}} = \sqrt{\frac{MwO_2}{MwN_2}} = \sqrt{\frac{32}{28}}$$

The calculated diffusion coefficients for N_2 at atmospheric pressure are given in Table 4.

Model Transposition from N_2 to CO_2

From the N_2 transport, it is again possible to transpose the model and to establish new equations for another respiratory gas: the CO_2.

The two first equations (in the gaseous compartments) remain identical in their structure:

$$\frac{dP_{CO_2Aw}}{dt} = \frac{\dot{V}}{V_{Aw}} P_{CO_2Air} - \frac{\dot{V} + K_{1CO_2}RT}{V_{Aw}} P_{CO_2Aw} + \frac{K_{1CO_2}RT}{V_{Aw}} P_{CO_2Alg} \qquad (1_{CO_2})$$

$$\frac{dP_{CO_2Alg}}{dt} = -\frac{RT}{V_{Alg}}(K_{1CO_2} + K_{2CO_2})P_{CO_2Alg} + \frac{RT}{V_{Alg}}\left[K_{1CO_2}P_{CO_2Aw} + K_{2CO_2}P_{CO_2Alb}\right] \qquad (2_{CO_2})$$

In the blood compartments, the situation is far more complex. Indeed, the CO_2 is present under three different states: a dissolved form, a form linked to the Hb (the carbaminohemoglobin), and as bicarbonate ions HCO_3^-. They represent approximately and, respectively, 7, 23, and 70% of the CO_2 carried by the blood stream, and the total concentration of CO_2 in the blood (C_{CO_2}) is given by the McHardy-Visser equation (29):

$$C_{CO_2} = \alpha_{CO_2} Pco_2 \left(1 + 10^{pH-pK}\right)\left(1 - \frac{0.0289\,[Hb]}{(3.352 - 0.456Sat)(8.142 - pH)}\right)$$

Hence, the total concentration of CO_2 in the blood is a function of the CO_2 solubility coefficient (α_{CO_2}), of the CO_2 partial pressure (Pco_2), of the equilibrium constant of the CO_2/HCO_3^- reaction (pK), of the hemoglobin concentration ([Hb]), the Hb saturation for oxygen (Sat), but also of an unknown parameter: the blood pH.

In the blood, the pH can be estimated by using two methods. First, the Henderson-Hasselbalch equation can be applied to the acid-base couple Pco_2/HCO_3^- and writes:

$$[HCO_3^-] = \alpha_{CO_2}\, Pco_2\, 10^{(pH-pK)}$$

Second, in the absence of metabolic disorder, the $[HCO_3^-]$ will be linearly linked to the pH along a line (of slope a) that passes through a point of coordinates pH = 7.4, $[HCO_3^-]$ = 24 mmol·L^{-1}. In a Davenport diagram (a representation of the $[HCO_3^-]$ as a function of the blood pH), it corresponds to the "buffer line" (30).

Hence,

$$[HCO_3^-] = a\,pH + b$$

with a = −21.6 mmol·L^{-1}/pH and b the coordinate at the origin (183.84 mmol·L^{-1}).

Hence, assuming there are no metabolic disorders, it is possible to conclude from the two previous equations that:

$$Pco_2 = g(pH) = \frac{a.\ pH + b}{\alpha_{CO_2} 10^{(pH-pK)}}$$

This function is bijective only into two distinct intervals of R^+ (]0;x0 [&] x0;+∞[) and its reciprocal function does not have any explicit expression. Nevertheless, in a physiological pH range, it is possible to establish $\hat{h}(Pco_2)$, an approximation of the reciprocal function of g and its derivative $\hat{h}(Pco_2)$(see Supplemental calculations S1).

$\hat{h}(Pco_2)$, an approximation of the reciprocal of g, is given by

$$pH = \hat{h}(Pco_2) = C_0 + C_1 lnPco_2 + C_2(lnPco_2)^2 + C_3(lnPco_2)^3 + C_4(lnPco_2)^4$$

And, considering that: $h'(Pco_2) = \frac{1}{g'(h(Pco_2))}$, $h'(Pco_2)$ its derivative writes:

Table 5. *Simulations performed to evaluate the model*

	Purpose of the Evaluation	Criteria	Conclusion
Normobaric steady state	O_2 model calibration	Adequation to ref. values	Validation of O_2 model in steady state
	CO_2 model calibration	Adequation to ref. values	Validation of the transposition process
Normobaric hyperoxic	O_2 model calibration	Adequation to ref. values	Validation of O_2 model in hypertoxic steady state
	N_2 model behavior description		Logical behavior
Normobaric static apnea	O_2 model calibration	Adequation to ref. values	Validation of O_2 model during dynamic changes
	CO_2 model behavior description		Logical behavior
Hyperbaric	O_2 model calibration	Adequation to ref. values	Validation of O_2 model in hyperbaric steady state
	N_2 model behavior description		Logical behavior

$$h'(Pco_2) = \frac{\alpha_{CO_2} 10^{(h(Pco_2)-pK)}}{a - (a\ h(Pco_2) + b)\ln 10}$$

It is now possible to express the total CO_2 concentration from a modified McHardy-Visser equation (Ψ) (29) as a function of Pco_2:

$$C_{CO_2} = \Psi(Pco_2) = \alpha_{CO_2} Pco_2 \left(1 + 10^{\hat{h}(Pco_2)-pK}\right) \times \left(1 - \frac{0.0289\,[Hb]}{(3.352 - 0.456\,Sat)\left(8.142 - \hat{h}(Pco_2)\right)}\right)$$

Similarly to what has been done for the O_2, as, in a given compartment i,

$$n_{CO_2 i} = V_i\ C_{CO_2 i}$$

it is possible to express the derivative of $n_{CO_2 i}$ as:

$$\frac{dn_{CO_2 i}}{dt} = Vi \frac{dP_{CO_2 i}}{dt} \Psi'(P_{CO_2 i})$$

with:

$$\Psi'(P_{CO_2 i}) = \alpha_{CO_2} \left[\left(\frac{-h'(P_{CO_2 i}) P_{CO_2 i}}{\left(8.142 - \hat{h}(P_{CO_2 i})\right)^2} \right) \left(1 + 10^{h(P_{CO_2 i})-pK}\right) + \left[1 - \frac{0.0289[Hb]}{\frac{3.352 - 0.456Sat}{8.412 - \hat{h}(P_{CO_2 i})}}\right] \left[1 + 10^{\hat{h}(P_{CO_2 i})-pk} \times (1 + P_{CO_2 i} \ln 10 \times h'(P_{CO_2 i}))\right] \right]$$

From these elements, it is now possible to establish the differential equations for the four blood compartments:

$$\frac{dP_{CO_2 Alb}}{dt} = \frac{1}{V_{Alb} \Psi'(P_{CO_2 Alb})} \left[K_{2CO_2} \left(P_{CO_2 Alg} - P_{CO_2 Alb}\right) + \dot{Q}\left(\Psi(P_{CO_2 v}) - \Psi(P_{CO_2 Alb})\right)\right] \quad (3_{CO_2})$$

$$\frac{dP_{CO_2 a}}{dt} = \frac{\dot{Q}}{V_a \Psi'(P_{CO_2 a})} \left[\Psi(P_{CO_2 Alb}) - \Psi(P_{CO_2 a})\right] \quad (4_{CO_2})$$

$$\frac{dP_{CO_2 c}}{dt} = \frac{1}{V_c \Psi'(P_{CO_2 c})} \left[\dot{Q}(\Psi(P_{CO_2 a}) - \Psi(P_{CO_2 c})) - K_{3CO_2}(P_{CO_2 c} - P_{CO_2 ti})\right] \quad (5_{CO_2})$$

$$\frac{dP_{CO_2 v}}{dt} = \frac{\dot{Q}}{V_v \Psi'(P_{CO_2 v})} \left[\Psi(P_{CO_2 c}) - \Psi(P_{CO_2 v})\right] \quad (6_{CO_2})$$

Regarding the calculation of the CO_2 partial pressure in the tissue compartment, the situation is simpler than in the blood compartment, as the carbon dioxide is only present in a dissolved state and as bicarbonate. The total CO_2 concentration can be expressed as:

$$C_{CO_2} = \alpha co_2 Pco_2 + (\alpha co_2 Pco_2 10^{(pH-pK)})$$

Considering again that the pH can be expressed from Pco_2 with the same function $pH = \hat{h}(Pco_2)$ used in the case of blood compartments, it is possible to rewrite the total CO_2 concentration:

$$C_{CO_2} = \Phi(Pco_2) = \alpha co_2 Pco_2 (1 + 10^{\hat{h}(Pco_2)-pK})$$

Leading to

$$\Phi'(Pco_2) = \alpha co_2 \left(1 + 10^{\hat{h}(Pco_2)-pk}\left(1 + Pco_2 (\ln 10) h'(Pco_2)\right)\right)$$

At last, it is here necessary to introduce the respiratory quotient (R_Q) defined as the ratio between the CO_2 production and the O_2 consumption rates:

$$R_Q = \frac{\dot{V}co_2}{\dot{M}o_2}$$

Finally, the differential equation describing the evolution of CO_2 in the tissue compartment writes:

$$\frac{dP_{CO_2 ti}}{dt} = \frac{1}{V_t \Phi'(P_{CO_2 ti})} \left[K_{3CO_2}(P_{CO_2 c} - P_{CO_2 ti}) + (R_Q \dot{M}O_2)\right] \quad (7_{CO_2})$$

Again, coefficients K_{1CO_2}, K_{2CO_2}, and K_{3CO_2} have been defined using the Graham's law:

$$\frac{K_{CO_2}}{K_{N_2}} = \sqrt{\frac{MwN_2}{MwCO_2}} = \sqrt{\frac{28}{44}}$$

The calculated diffusion coefficients for CO_2 at atmospheric pressure are given in the Table 5.

Model Evaluation

Normobaric steady-state simulation.
In the first step, the model is evaluated in a steady state at atmospheric pressure with an O_2 fraction corresponding to the ambient air. In this condition, the model is supposed to reach a steady state at the physiological O_2 partial pressures.

Normobaric hyperoxic simulation.
In a second phase, after 20 min of steady state, a 20-min exposure to pure O_2 followed by a return to air breathing is simulated. Modifications in O_2 and N_2 partial pressures in alveolar gas, arterial blood, venous blood, and tissue compartment were calculated as well as the time constant for these compartments ($t_{1/2}$). After an instantaneous change in the partial pressure of a gas in the breathing mixture (the ambient air), the partial pressure of this gas will change in the different compartments of the model to reach a new steady state. The $t_{1/2}$ in a given compartment is defined as the time needed for a gas partial pressure to reach 50% of its new value. It is important to note that here, the $t_{1/2}$ are calculated from the gas partial pressure evolution and not defined a priori.

Normobaric static apnea simulation.
To go on with the analysis of the model numerical behavior, after 20 min of steady state, the ventilatory flow is stopped (set to 0) during a period of 2 min and then restored at 8.1 $L \cdot min^{-1}$. The simulation is made with $\dot{Q}$ = $L \cdot min^{-1}$ and assuming an initial hyperventilation before the apnea (at 16 $L \cdot min^{-1}$ during 0.2 min) and of a 1-min ventilatory response after the apnea (ventilatory flow: 50 $L \cdot min^{-1}$). The results are compared with published data (31).

Table 6. *Computed P_{O_2}, P_{CO_2}, and pH in normobaric condition*

Compartment	P_{O_2}, kPa	P_{CO_2}, kPa	pH
Airways	17.3	1.9	
Alveolar gas	13.9	4.6	
Arterial blood	12.8	5.5	7.39
Venous blood	5.3	6.5	7.34
Tissues	2.0	9.2	7.23

Hyperbaric simulation.

After 20 min of steady-state simulation, the ambient pressure is increased at 20 kPa·min^{-1} to 192 kPa (1.9 ATA) and kept constant until $t = 40$ min when the pressure is increased again at the same speed to 253 kPa (2.5 ATA). At $t = 60$ min, the pressure is then reduced (at 20 kPa·min^{-1}) to ambient pressure. Gas pressure is simulated in all compartments.

The calculated P_{O_2a} (as a function of ambient P_{O_2}) are compared with values from the literature (32–34).

The different simulations and their purpose are summarized in Table 5.

All the simulations are performed using a Runge-Kutta 4 discretization method with a time step (*dt*) of 1/1,000 of minute over a period of 100 min. Spearman analysis is performed to evaluate the correlation between calculated and reference values (Statistica 15).

RESULTS

Steady-State Normobaric Simulation

The simulation of the O_2 transfer from ambient air at atmospheric pressure to the tissues enabled to compute the different aforementioned O_2 partial pressures. For an atmospheric pressure of 101.3 kPa and an O_2 fraction of 0.21, the obtained O_2 partial pressures stabilized at values included in their physiological ranges (see Fig. 2 and Table 6). A Spearman analysis showed a correlation coefficient R between calculated and reference values of 0.997 and a highly significant *P* value ($P < 0.01$). The N_2 partial pressure stabilized at 75.1 kPa in all the calculated compartments. As there is no metabolic consumption or production, this N_2 partial pressure corresponds to the P_{N_2} in air saturated with vapor pressure.

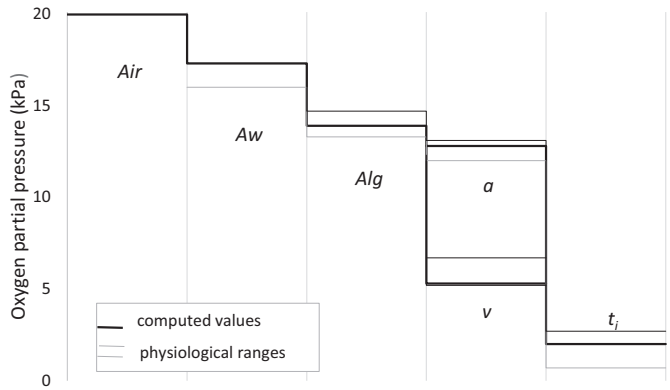

Figure 2. Oxygen cascade (physiological ranges and computed values). a, arterial compartment; Alg, alveolar gas compartment; Aw, airways compartment; ti, tissue compartment; v, venous compartment.

Table 7. *Oxygen and nitrogen $t_{1/2}$ during hyperoxia exposure*

	$t_{1/2}$ P_{AW}	$t_{1/2}$ P_{Alg}	$t_{1/2}$ P_a	$t_{1/2}$ P_v	$t_{1/2}$ P_t
Oxygen	10.3 s	21.4 s	49.2 s	1 min 54 s	1 min 26 s
Nitrogen	10.6 s	20.8 s	44.6 s	22 min 34 s	20 min 8 s

In the N_2 model, all the partial pressures equilibrated with the ambient air at 75.1 kPa.

The computed P_{CO_2} values are given in Table 6 together with the corresponding pH determined with the equation h(Pco_2). The correlation ($R^2 = 0.792$, $P = 0.04$) between these computed P_{CO_2} and literature values (32, 35, 36) was possible for alveolar gas, arterial blood, and venous blood. Furthermore, the computed pH values were in very good accordance with reference physiological values.

Normobaric Hyperoxic Simulation

The evolutions of the calculated O_2 and N_2 partial pressures during a normobaric exposure to pure oxygen and a return to normoxia are presented in the Fig. 3. During the 20-min hyperoxia exposure, the oxygen pressures stabilized at 92.4 kPa in the airways, 89.1 kPa in the alveolar gas, 87.7 kPa in the arterial blood, 8.7 kPa in the venous blood, and 3.7 kPa in the tissue compartment. For the gaseous compartments and arterial partial pressure, there is a rapid change in partial pressure, in the case of tissue and venous compartments, the kinetics are a little bit slower as shown by the $t_{1/2}$ (see Table 7). In the N_2 case, breathing pure O_2 resulted in a sharp decrease of all P_{N_2}. The 20-min oxygen exposure was nevertheless not sufficient to stabilize even the faster gaseous compartments and $t_{1/2}$ for venous and tissue compartments are, respectively, of 17.05 and 19.10 min (Table 7). Regarding carbon dioxide, breathing pure O_2 did not induce any noticeable changes in the computed P_{CO_2}(data not shown).

Normobaric static apnea simulation.

Inducing an apnea via a stop of the respiration induces a rapid fall of O_2 partial pressure in the gaseous compartments (see Fig. 4*A*). This evolution is smoother in the arterial blood and the lower Pa_{O_2} (6.6 kPa) is observed 3 s after the end of the apnea. In the tissue and venous blood, the minimal O_2 partial pressures were 0.65 kPa and 5.2 kPa, respectively, 20 s and 5 s after the end of the simulated apnea. During the apnea, the P_{O_2a} were fitting closely to data from Gardette and Plutarque (31) (Spearman test $P < 0.01$, see Fig. 4*C*). Rather logically, these apnea simulations did not have any effect on P_{N_2}, whatever the considered compartment (results not shown). On the contrary, P_{CO_2} were strongly increased during the apnea (see Fig. 4*B*); in the gaseous compartment, the P_{CO_2} were sharply increased while apnea effects were moderate in the blood compartments and not noticeable in the tissue compartment. Interestingly, pre and post apnea hyperventilation had clear effects on both O_2 and CO_2 partial pressures.

Hyperbaric Simulation

The increase in ambient pressure had a direct effect on O_2 and N_2 partial pressures in the ambient air. For the oxygen partial pressures (see Fig. 5*A*), the 1.9 and 2.5 ATA stops lead (after a transient phase nearly parallel to the change of air

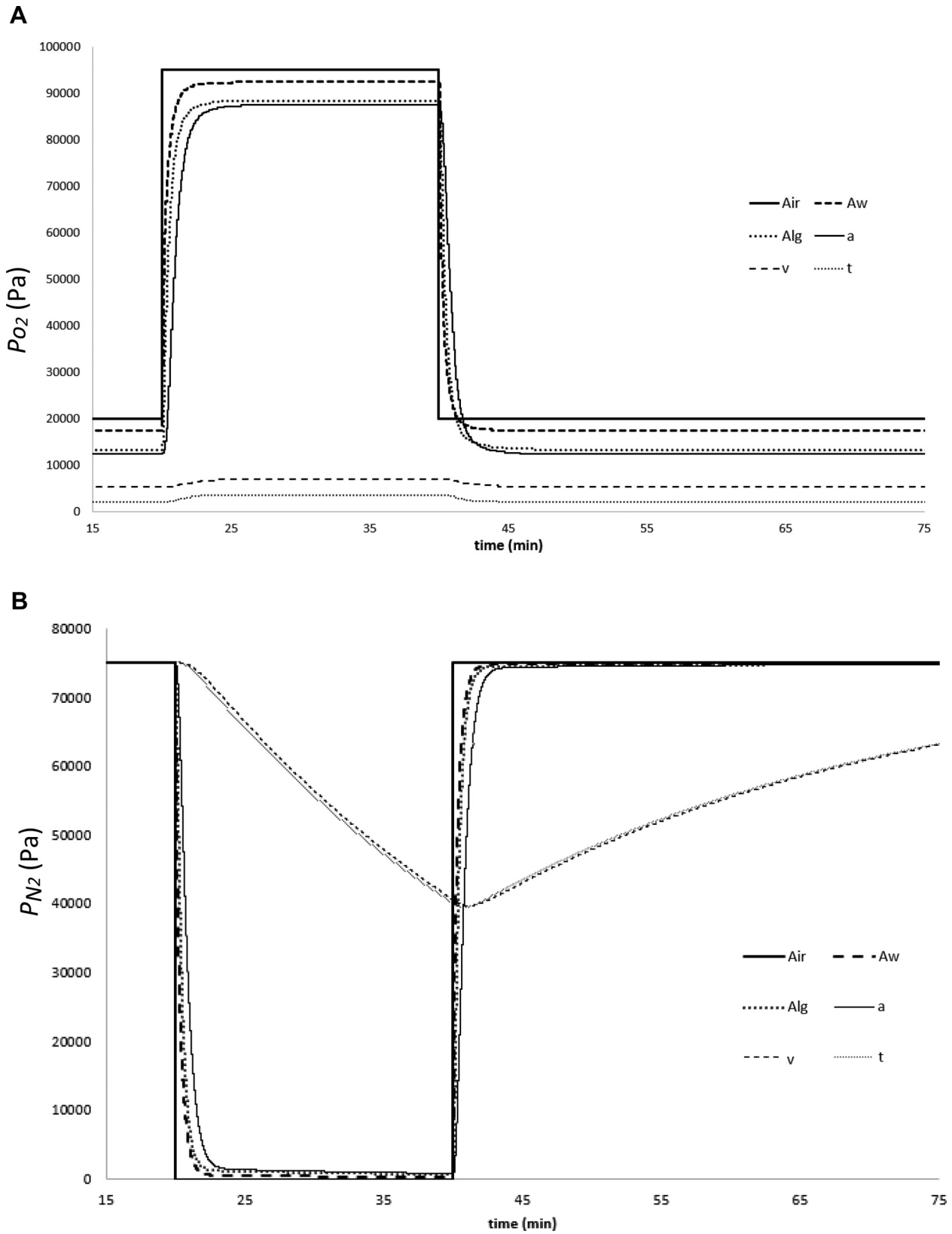

Figure 3. Normobaric hyperoxic simulation: N_2 and O_2 partial pressures. *A*: O_2. *B*: N_2. a, arterial compartment; Alg, alveolar gas compartment; Aw, airways compartment; t, tissue compartment; v, venous compartment.

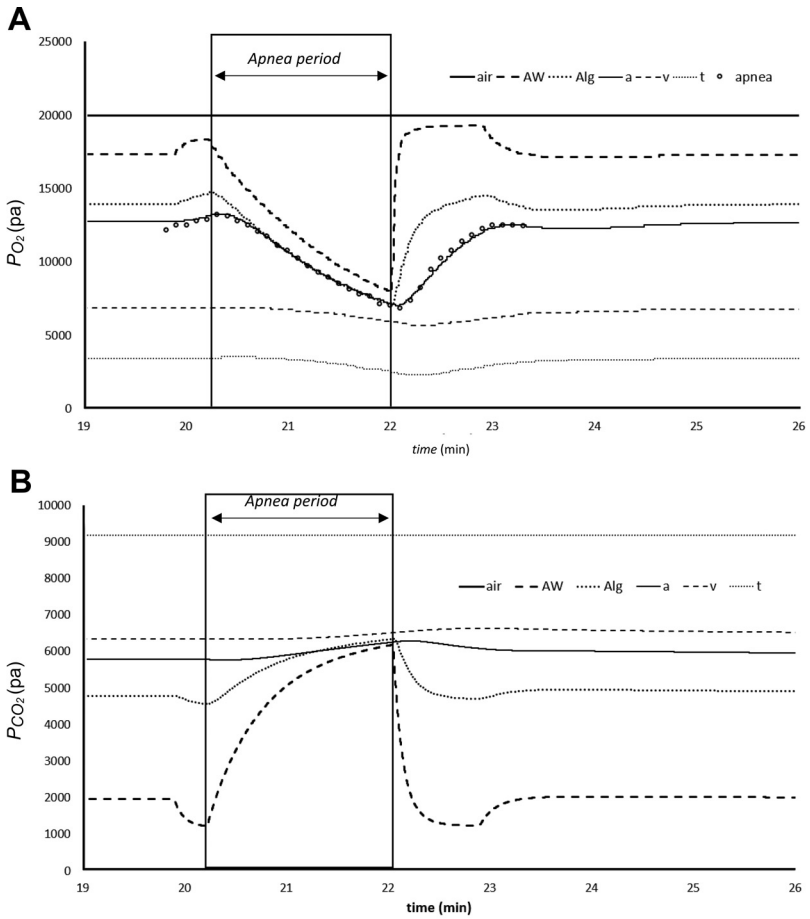

Figure 4. Normobaric static apnea simulation. *A*: N_2 partial pressures. *B*: O_2 partial pressures. *C*: correlation between observed $TcPo_2$ and Pa_{O_2} computed values. a, arterial compartment; Alg, alveolar gas compartment; Aw, airways compartment; t, tissue compartment; v, venous compartment; open circles in Fig. 4*A* correspond to Po_2 measured before during and after apnea.

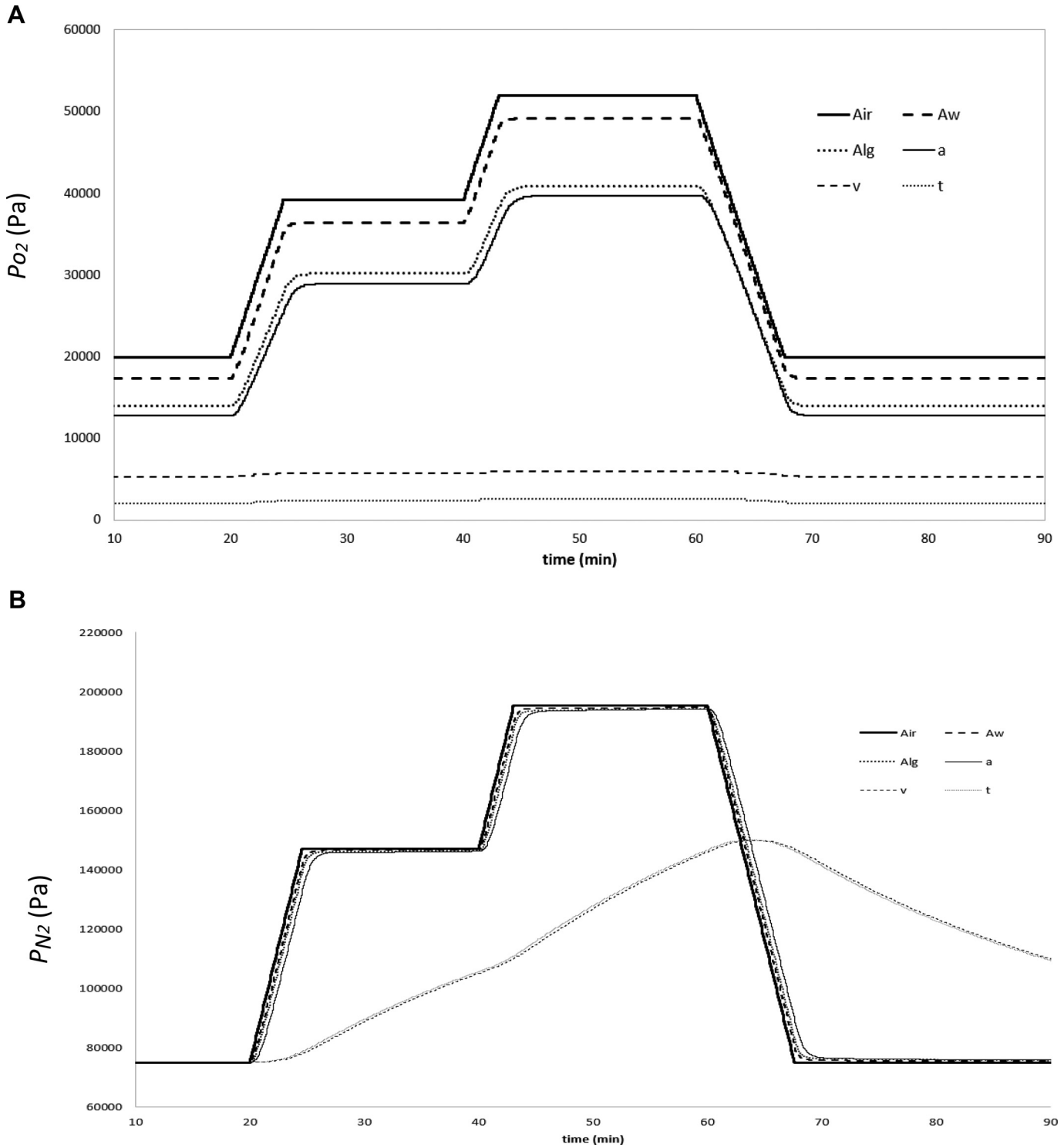

Figure 5. Hyperbaric simulation, nitrogen, and oxygen partial pressures. *A*: oxygen. *B*: nitrogen. a, arterial compartment; Alg, alveolar gas compartment; Aw, airways compartment; t, tissue compartment; v, venous compartment.

P_{O_2}) to steady states for all the considered compartments. For P_{O_2a}, these steady states can be compared (see Fig. 6) with data from the literature (32–34). The results of the model computations appear to be close to the available values at least up to an ambient P_{O_2} of 86 kPa. Nevertheless, at an ambient P_{O_2} of 101 kPa, and without any cardiovascular adaptation to hyperoxia, the model seems to overevaluate the P_{O_2a} when compared with the data of Whalen (32) and Smit (34).

For the nitrogen partial pressures, the situation appears to be different. In venous and tissue compartments (in Fig. 5*B*), N_2 pressure increases slowly. In arterial blood and alveolar gas, a rapid increase in P_{N_2} during the ambient pressure rise

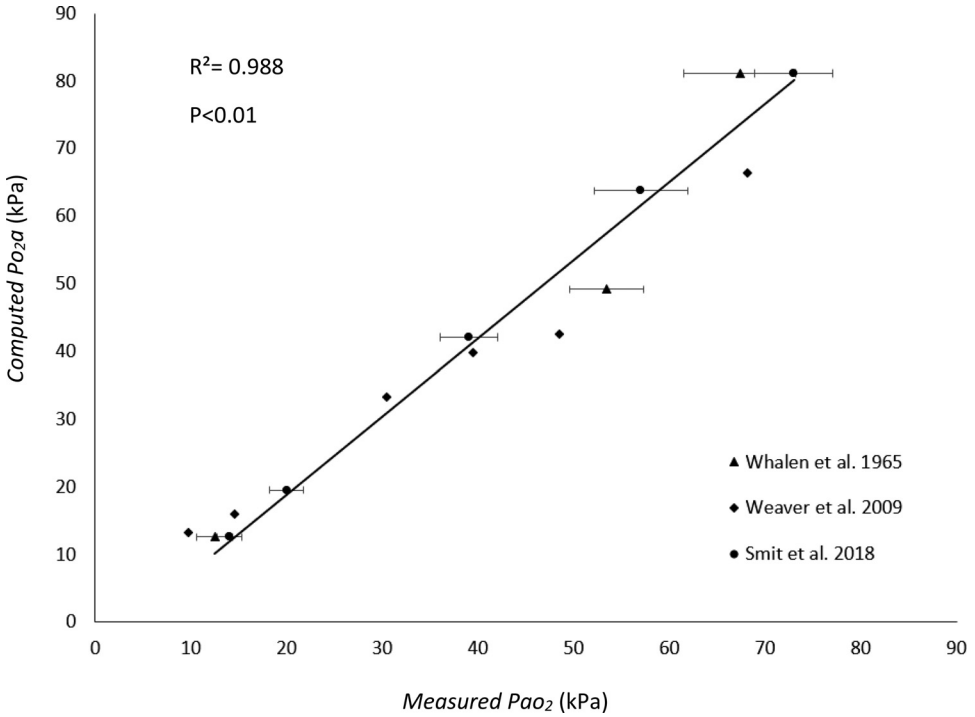

Figure 6. Hyperbaric simulation, correlation between observed and computed Pa_{O_2} values. a, arterial compartment; Alg, alveolar gas compartment; Aw, airway compartment; t, tissue compartment; v, venous compartment.

is followed by a slower evolution of P_{N_2} that converges to the ambient P_{N_2}.

In these conditions P_{CO_2} were not modified whatever the compartment.

DISCUSSION

Decompression Modeling

The stages of gas transport to the tissues are ventilatory convection, alveolar-capillary diffusion, blood convection, and tissue diffusion. As the work of Haldane (7), the first stages (from ventilated gases to arterial blood) have been considered almost instantaneous and therefore negligible for the analysis of gas exchange dynamics during diving. The focus is thus on the delivery of gases by the blood circulation to the capillary beds and their diffusion from the capillaries to the tissues.

The delivery of an inert gas through perfusion to the organs and tissues primarily depends on its solubility (Henry's law) and on the perfusion rate (which varies depending on the tissue and over time). Thus, it is considered that well-perfused tissues (liver, kidney, brain, and heart) saturate and desaturate more rapidly than poorly perfused tissues (fat). Mack and Lin (37) showed in an in vivo experimental model that increasing the cardiocirculatory gas transport capacity (cardiac output and tissue perfusion) increases the rate of N_2 elimination by the slowest compartments. Aukland et al. (38) established that changes in the amount of a gas in a tissue depends on the arterio-venous differential of that gas and on the perfusion rate of the tissue.

The issue of gas diffusion between capillaries and tissues is extremely complex and varies according to the tissues. Indeed, this diffusion rate from the capillary bed to the associated tissue is not only proportional to the partial pressure differential of the gas but also depends on the diffusion coefficient of the gas at the interface between the blood and the tissue and within the tissue. These coefficients themselves depend on the architecture and properties of the exchanger (39).

Given the complexity of the various factors involved in gas transfer to the tissues, Haldane's solution (7) was to propose compartments, completely independent from each other's, and defined by a half-saturation time. This solution has the advantage of simplicity (the processes we previously considered are ignored), but it leaves unanswered the question of the weight of the physiological parameters involved in gas exchange rates. This simplification is the origin of the development of the Haldanian and Bühlmann's monoexponential models widely and efficiently used for decades in decompression management.

Although compartments are sometimes identified with tissues or organs, experimental data indicate that even at the scale of a tissue as bone marrow (40), brain, or skeletal muscle (41), the kinetics of gas exchange are more often better described by multiexponential models (and therefore, theoretically several compartments) than by monoexponential models.

As discussed earlier, the relationship between diffusion and perfusion in models of gas transport has been a subject of investigation over several decades, and the modeling of the gas exchange to the tissues was initially based on the premise proposed by Haldane that the structures of the tissue exchangers are optimized to promote diffusion and thus implies that diffusion is not limiting. However, different works to assess blood flows in different tissues (using the Fick principle and different gases: Kr, H_2, Xe, etc.) show that the hypothesis of limiting gas exchange based solely on perfusion is insufficient to accurately account for their experimental results (42, 43). Hennessy (44) further explored the interaction between diffusion and perfusion, concluding that

Haldane's approach remains an insufficient approximation even when approaching stable states (asymptotic states). However, Ohta et al. (45) suggested that diffusion played a negligible role in argon-to-tissue exchange. More recently, research by Doolette et al. (46) involving helium demonstrated that in vivo results in sheep were better explained by a perfusion-diffusion model rather than a perfusion model. In addition, Murphy et al. (47, 48) underscored the significance of considering diffusion phenomena for predicting decompression sickness. The model presented here is as far as we know, the only one that integrates both diffusive and convective aspects involved in O_2 transport, to propose a set of differential equations of respiratory and inert gases.

Diffusive Parameters

Our model is based on the assumption of homogenous compartments connected through gas exchanges driven by different convective and diffusive steps. The determination of physiological constants significantly differs in these two cases. Convective parameters can be readily found in the literature, encompassing respiratory and blood volumes, flows (25, 49), and solubility coefficients (26, 50). On the other hand, determining diffusion coefficients is a more complex problem. These coefficients are inherently dependent on the architecture of gas exchangers, as well as the intrinsic permeability of tissues. The intricate nature of lung and tissue diffusion, characterized by vascular heterogeneity, various tissue architectures, and composition, poses significant challenges. Our approach offers a solution by using differential equations describing each diffusive step and leveraging knowledge about the stable states of the O_2 transport steps. For example, in the case of alveolo-capillary diffusion, *Eq. 3* and a stable state (where all oxygen partial pressures are constant, $\frac{dP}{dt} = 0$) enable us to determine the global diffusion coefficient for the specific step. Similarly, within a given tissue, this approach makes it possible to determine diffusion coefficients based on the tissue's O_2 consumption rate, O_2 partial pressure, and P_{O_2c}. Given that these parameters are either available in the literature or can be measured experimentally, our approach offers the potential to derive diffusion coefficients for any organ of interest in the context of decompression. It is noteworthy that in this manuscript, various O_2 diffusion coefficients were derived from a range of reference P_{O_2} values, leading to considerable ranges of possible coefficients. A promising avenue for future research involves applying this method to an individual's unique set of physiological values.

Model Validation

The validity of our oxygen exchange model has been assessed across multiple scenarios, encompassing stable states, normoxia, hyperoxia (both normobaric and hyperbaric), and static apnea. In normoxic conditions (at the atmospheric pressure with an oxygen fraction in dry air of 0.21), the calculated oxygen partial pressures across different compartments align with established physiological values. Strong and significant correlations between the calculated and observed values ($R^2 = 0.997$, $P < 0.01$) underscore the model's ability to replicate key aspects of oxygen transport. In this condition, all P_{N_2} stabilize at 75.1 kPa: the nitrogen partial pressure in the air when saturated with water. A second step of the model evaluation has been the calculation of the gas partial pressures in the context of a normobaric simulation of pure oxygen breathing. During the 20-min of simulated hyperoxia, the stabilization of the calculated oxygen partial pressure was rapid (with $t_{1/2}$ of few tens of seconds) in all compartments. In the case of nitrogen, the simulation of pure oxygen breathing induces a rapid decrease of all P_{N_2}. The stabilization of the tissue and the venous compartment was slower than in the case P_{O_2} and their measured time of half desaturation were 20 min 8 s and 22 min 34 s, respectively. It is important to note that, in this simulation, the half desaturation times are not a priori inputs of the model as they usually are in the algorithms computing decompression profiles, but they are the result of the architecture of the model and of the physiological values used (ventilatory flow, cardiac output, diffusion coefficients ….). In the case of this model with one compartment integrating all the organs and tissues, the obtained $t_{1/2}$ is close to 20 min. This value falls within the range of the admitted half-time (ranging nevertheless from a few minutes to several hundred minutes).

Another evaluation of the behavior of the model has been performed simulating a static apnea. The interruption of the ventilator flow induced a rapid fall of P_{O_2} in all computed compartments. These results were compared with data from previous experiments (31). As physiological volumes and flows were not available, it has not been possible to implement the pre and postapnea hyperventilation in the model. The model has consequently been set making assumptions on these variables. Again, complementary experiments would be necessary to measure the physiological variables needed by the model, but the obtained results show that this model enables to reproduce correctly the evolution of arterial P_{O_2} during a static apnea ($R^2 = 0.991$, $P < 0.01$).

The last step of evaluation of the oxygen model has been performed simulating hyperbaric conditions. Increasing the ambient pressure has, very logically, induced P_{N_2} and P_{O_2} increases in all the compartments of the model. The comparison of the calculated P_{O_2a} and data from the literature show that there is a very good correlation between these two variables up to an air P_{O_2} of 86 kPa. Nevertheless, a small divergence seems to appear when the model results are compared with the data from Whalen (32) and Smit (34) at an ambient P_{O_2} of 101 kPa. This point will require further investigations if the model is to be used in the context of high-inspired P_{O_2}, but the validity of this model is good ($R^2 = 0.988$, $P < 0.001$) and its range is compatible with the analysis of most of the recreational dives.

The approach presented in this manuscript is based on three distinct steps. The first step consists in building a model of oxygen transfer that has the advantage of being based on the large amount of knowledge on the physiology of this gas. The second step is the transposition of this model to the case of nitrogen, the inert gas involved in DCS. A limit of this approach is that it is based on the hypothesis that the O_2 model (and in particular the diffusion coefficients) can be transposed to nitrogen. This assumption appears not to be always true and for example, the differences between nitrogen and helium pharmacokinetics (generally assumed) are not always confirmed by experimental measurement (41). To evaluate the validity of the transposition process, the nitrogen model has been again transposed to another well-known gas: the carbon dioxide. Hence, a third step has been performed and the CO_2

model has been built from the N_2 model. Despite these two transposition processes, despite the complexity of the P_{CO_2} equation set and despite the simplification hypothesis needed to compute the total CO_2 (the model is not valid in case of metabolic acid-base disorders), the resulting model spontaneously stabilizes at physiological alveolar gas, arterial and venous P_{CO_2}, and reproduces with a very satisfying exactitude arterial and venous pH. From these results, we conclude that the transposition procedure from a gas to another is valid and hence that the validity of the nitrogen model is highly plausible. A more direct validation of the N_2 model based on measurements of nitrogen exchanges will nevertheless be necessary.

Model Architecture

It is important to note that, in our model's current configuration, arterial and alveolar blood P_{O_2} are nearly equal. The same observation can be made between the tissue capillary bed and the venous compartment. Consequently, and to make the different results easier to read, the P_{Alb} and the P_c are not presented in the different figures and tables of this manuscript. This equivalence arises from our consideration of alveolar capillaries as a single homogeneous compartment supplying arterial blood exclusively. Notably, factors like the foramen ovale (a physical connection between the right and left atria) and pulmonary shunts (blood bypassing the lungs without gas exchange) have not been integrated into the model. These physiological phenomena lead to mixing of venous blood with oxygenated blood in the pulmonary veins or left atrium, resulting in lower arterial P_{O_2a} compared with P_{O_2Alb}. These shunts of the pulmonary function can easily be added in the present model by modifying *Eqs. 3* and *4* to send a fraction of the blood flow directly from the venous compartment to the arterial one. There is a potentially strong interest in integrating these shunts in a physiological model of decompression as they are known to increase the risk of DCS (51–53). Considering capillary bed and venous compartment, in vivo, the P_{O_2} in the vena cava results from the mixing of the different venous blood either strongly oxygenated (from the renal blood flow) or with low P_{O_2} (from hepatic vein or active skeletal muscles). In addition, while our model currently represents one tissue with one capillary bed, further development should involve the inclusion of different tissues to accurately capture the dynamics of gas exchange across tissues relevant to decompression scenarios in the context of DCS prevention.

Conclusions

The major interest of the model presented here is to pave the way for the integration of physiological and morphological elements in a model of gas saturation/desaturation. Contrary to Haldanian-type models including Bühlmann-type models, the model presented here is not solely based on the evolution of partial pressures of gases, but is designed to describe the transfer of gas quantities. It can therefore quantify how the diver takes on inert gas during the dive and how this gas is eliminated during the ascent to the surface on a quantitative basis. This model also opens the possibility to integrate different tissues, patent foramen ovale, or pulmonary shunts and to calculate their influence on the global kinetics of N_2 elimination. This model could also integrate data on the cardio/respiratory activity during a dive. It could enable the integration of the physiological state of the diver before and during the dive in the decompression algorithms and consequently to individualize the decompression process. This manuscript is only a first step toward the integration of physiological parameters in a decompression algorithm and further developments are clearly needed to make this model useful. Bubble modeling could be interesting to introduce in circulating and tissue compartments, and relevant tissue compartments will have to be defined on the basis of the physiology of gas exchanges and the physiopathology of DCS.

GLOSSARY

a	Arterial compartment
Alb	Alveolar blood compartment
Alg	Alveolar gas compartment
AP	Ambient Pressure (in Pa)
Aw	Airways compartment
c	Capillary blood compartment;
C_{x_2i}	Concentration of gas x in compartment i (in mmol·L^{-1})
fro_2	Fraction of oxygen in a gas mix (without unit)
[Hb]	Hemoglobin concentration (in mmol·L^{-1})
K_{1x}	Diffusion coefficient of gas x at the interface between the airways and the alveolar gas (in mmol·min^{-1}·Pa^{-1})
K_{2x}	Diffusion coefficient of gas x at the interface between the alveolar gas and the alveolar blood (in mmol·min^{-1}·Pa^{-1})
K_{3x}	Diffusion coefficient of gas x at the interface between the capillary blood and the corresponding tissue (in mmol·min^{-1}·Pa^{-1})
$\dot{M}_{O_2}$	Oxygen consumption rate (in mmol·min^{-1}.kg^{-1})
n_{xi}	Quantity of gas x in compartment i (in mmol)
Oxc	Oxygen carrying capacity of hemoglobin (in mL·g^{-1})
P_{H_2O}	Water vapor partial pressure at 37 °C (6,246 Pa)
P_{xi}	Partial pressure of gas x in compartment i (in Pa);
$\dot{Q}$	Cardiac blood flow (in L·min^{-1})
$\dot{Q}_i$	Blood flow in a given tissue (in L·min^{-1})
R	Ideal gas constant (8.314 J·mol^{-1}·K^{-1})
R_Q	Respiratory quotient
Sat	Hemoglobin saturation (in %)
t	Time (in min)
T	Absolute temperature (in K, approximately 310°K in the human body)
ti	Tissue compartment
TcP_{O_2}	Transcutaneous oxygen partial pressure (Pa)
v	Venous compartment;
$\dot{V}$	Ventilatory flow (in L·min^{-1})
$\dot{V}_{CO_2}$	CO_2 production rate (in mmol·min^{-1}·kg^{-1})
V_i	Volume of compartment i (in L)
α_{xi}	Solubility of gas x in compartment i (in mmol·L^{-1}/Pa)

DATA AVAILABILITY

Data will be made available upon reasonable request.

SUPPLEMENTAL MATERIAL

Supplemental calculations S1: https://hal.science/hal-04722226.

GRANTS

This research received a grant from MedSupHyp, the French "Société de Medicine Subaquatique et Hyperbare."

DISCLOSURES

No conflicts of interest, financial or otherwise, are declared by the authors.

AUTHOR CONTRIBUTIONS

M.T., A.B., L.N., P.B., F.G., and J.-P.P. conceived and designed research; M.T., A.B., B.G., A.H., and J.-P.P. analyzed data; M.T., A.B., E.D., B.G., A.H., and J.P. interpreted results of experiments; M.T., A.B., and B.G. prepared figures; M.T., A.B., and E.D. drafted manuscript; M.T., A.B., and F.G. edited and revised manuscript; M.T., A.B., B.G., and F.G. approved final version of manuscript.

REFERENCES

1. **Cialoni D**, **Pieri M**, **Balestra C**, **Marroni A.** Dive risk factors, gas bubble formation, and decompression illness in recreational SCUBA diving: analysis of DAN Europe DSL Data Base. *Front Psychol* 8: 1587, 2017. doi:10.3389/fpsyg.2017.01587.
2. **Hemelryck W**, **Germonpré P**, **Papadopoulou V**, **Rozloznik M**, **Balestra C.** Long term effects of recreational SCUBA diving on higher cognitive function. *Scand J Med Sci Sports* 24: 928–934, 2014. doi:10.1111/sms.12100.
3. **Wienke B**, **O'Leary T.** Downs and ups of decompression diving: a review. *MAOPS* 3, 2019. doi:10.32474/MAOPS.2019.03.000154.
4. **Gempp E**, **Blatteau J-E.** Preconditioning methods and mechanisms for preventing the risk of decompression sickness in SCUBA divers: a review. *Res Sports Med* 18: 205–218, 2010. doi:10.1080/15438627.2010.490189.
5. **Germonpré P**, **Balestra C.** Preconditioning to reduce decompression stress in SCUBA divers. *Aerosp Med Hum Perform* 88: 114–120, 2017. doi:10.3357/AMHP.4642.2017.
6. **Imbert J-P**, **Egi SM**, **Germonpré P**, **Balestra C.** Static metabolic bubbles as precursors of vascular gas emboli during divers' decompression: a hypothesis explaining bubbling variability. *Front Physiol* 10: 807, 2019. doi:10.3389/fphys.2019.00807.
7. **Boycott AE**, **Damant GCC**, **Haldane JS.** The prevention of compressed-air illness. *J Hyg (Lond)* 8: 342–443, 1908. doi:10.1017/S0022172400003399.
8. **Hugon J.** Decompression models: review, relevance and validation capabilities. *Undersea Hyperb Med* 41: 531–556, 2014.
9. **Rees SE**, **Andreassen S.** Mathematical models of oxygen and carbon dioxide storage and transport: the acid-base chemistry of blood. *Crit Rev Biomed Eng* 33: 209–264, 2005 [Erratum in *Crit Rev Biomed Eng* 35: 443–445, 2007]. doi:10.1615/CritRevBiomedEng.v33.i3.10.
10. **Mountain JE**, **Santer P**, **O'Neill DP**, **Smith NMJ**, **Ciaffoni L**, **Couper JH**, **Ritchie GAD**, **Hancock G**, **Whiteley JP**, **Robbins PA.** Potential for noninvasive assessment of lung inhomogeneity using highly precise, highly time-resolved measurements of gas exchange. *J Appl Physiol (1985)* 124: 615–631, 2018. doi:10.1152/japplphysiol.00745.2017.
11. **Magor-Elliott SRM**, **Fullerton C**, **Richmond G**, **Ritchie GAD**, **Robbins PA.** A dynamic model of the body gas stores for carbon dioxide, oxygen, and inert gases that incorporates circulatory transport delays to and from the lung. *J Appl Physiol (1985)* 130: 1383–1397, 2021. doi:10.1152/japplphysiol.00764.2020.
12. **Workman RD.** Calculation of decompression schedules for nitrogen -oxygen and helium-oxygen dives. *Res US Navy Exp Diving Unit* 26: 1–33, 1964. doi:10.21236/ad0620879.
13. Decompression: Decompression Sickness - Buhlmann, A.A.: 9780387133089 - AbeBooks [Online]. [date unknown]. https://www.abebooks.fr/9780387133089/Decompression-Sickness-Buhlmann-A.A-0387133089/plp [16 Aug. 2024].
14. **Meliet JL**, **Mayan PY.** Le pronostic des accidents de décompression dans la Marine Nationale: influence du délai d'apparition et du délai de recompression. *MedSubHyp* 9: 63–75, 1990.
15. **Hempleman HV.** Investigation into the decompression tables: a new theoretical basis for the calculation of decompression tables. Royal Naval Personnel Research Committee, Report III – Part A, UPS131, Medical Research Council, London: 1952.
16. **Hills BA.** A thermodynamic and kinetic approach to decompression sickness.
17. **Hennessy TR.** On the site of origin, evolution and effects of decompression microbubbles. In: Supersaturation and Bubble Formation in Fluids and Organisms.
18. **Chappell MA**, **Payne SJ.** A physiological model of the release of gas bubbles from crevices under decompression. *Respir Physiol Neurobiol* 153: 166–180, 2006. doi:10.1016/j.resp.2005.10.006.
19. **Hugon J.** Vers une modélisation biophysique de la décompression [Online]. Aix-Marseille 2: 2010. https://theses.fr/2010AIX20691 [21 Aug. 2024].
20. **Severinghaus JW.** Simple, accurate equations for human blood O2 dissociation computations. *J Appl Physiol Respir Environ Exerc Physiol* 46: 599–602, 1979. doi:10.1152/jappl.1979.46.3.599.
21. **Stahl WR.** Scaling of respiratory variables in mammals. *J Appl Physiol* 22: 453–460, 1967. doi:10.1152/jappl.1967.22.3.453.
22. **Quanjer PH**, **Stanojevic S**, **Cole TJ**, **Baur X**, **Hall GL**, **Culver BH**, **Enright PL**, **Hankinson JL**, **Ip MSM**, **Zheng J**, **Stocks J**; **the ERS Global Lung Function Initiative.** Multi-ethnic reference values for spirometry for the 3–95-yr age range: the global lung function 2012 equations. *Eur Respir J* 40: 1324–1343, 2012. doi:10.1183/09031936.00080312.
23. **Vital Durand D**, **Le Jeune C.** *DOROSZ* 37th Ed. Weaver. Maloine, 2018.
24. **Dijkhuizen P**, **Buursma A**, **Fongers TME**, **Gerding AM**, **Oeseburg B**, **Zijlstra WG.** The oxygen binding capacity of human haemoglobin. *Pflugers Arch* 369: 223–231, 1977. doi:10.1007/BF00582188.
25. **Guillien A**, **Soumagne T**, **Regnard J**, **Degano D**; **Group Fonction de la SPLF.** [The new reference equations of the Global Lung function Initiative (GLI) for pulmonary function tests]. *Rev Mal Respir* 35: 1020–1027, 2018. doi:10.1016/j.rmr.2018.08.021.
26. **Battino R**, **Rettich TR**, **Tominaga T.** The solubility of nitrogen and air in liquids. *Journal of Physical and Chemical Reference Data* 13: 563–600, 1984. doi:10.1063/1.555713.
27. **Christmas KM**, **Bassingthwaighte JB.** Equations for O_2 and CO_2 solubilities in saline and plasma: combining temperature and density dependences. *J Appl Physiol (1985)* 122: 1313–1320, 2017. doi:10.1152/japplphysiol.01124.2016.
28. **Altman PL**, **Dittmer DS.** *Biology Data Book*, 3rd Ed. Federation of American societies for experimental biology. Bethesda, Maryland: 1974.
29. **Douglas AR**, **Jones NL**, **Reed JW.** Calculation of whole blood CO2 content. *J Appl Physiol (1985)* 65: 473–477, 1988. doi:10.1152/jappl.1988.65.1.473.
30. **Cherniack NS**, **Longobardo GS.** Oxygen and carbon dioxide gas stores of the body. *Physiol Rev* 50: 196–243, 1970. doi:10.1152/physrev.1970.50.2.196.
31. **Gardette B**, **Plutarque M.** *COMEX 50 ans de recherches et d'innovations*. Club des anciens de la COMEX. Marseille, France: 2012.
32. **Whalen RE**, **Saltzman HA**, **Holloway DH**, **McIntosh HD**, **Sieker HO**, **Brown IW.** Cardiovascular and blood gas responses to hyperbaric oxygenation. *Am J Cardiol* 15: 638–646, 1965. doi:10.1016/0002-9149(65)90350-4.
33. **Weaver LK**, **Howe S**, **Snow GL**, **Deru K.** Arterial and pulmonary arterial hemodynamics and oxygen delivery/extraction in normal humans exposed to hyperbaric air and oxygen. *J Appl Physiol (1985)* 107: 336–345, 2009 [Erratum in *J Appl Physiol (1985)* 124: 1385, 2018]. doi:10.1152/japplphysiol.91012.2008.
34. **Smit B**, **Smulders YM**, **Eringa EC**, **Gelissen HPMM**, **Girbes ARJ**, **De Grooth HS**, **Schotman HHM**, **Scheffer PG**, **Oudemans-van Straaten HM**, **Spoelstra-de Man AME.** Hyperoxia does not affect oxygen delivery in healthy volunteers while causing a decrease in sublingual perfusion. *Microcirculation* 25: e12433, 2018. doi:10.1111/micc.12433.
35. **Lambertsen CJ**, **Kough RH**, **Cooper DY**, **Emmel GL**, **Loeschcke HH**, **Schmidt CF.** Comparison of relationship of respiratory minute volume to pCO2 and pH of arterial and internal jugular blood in normal man during hyperventilation produced by low concentrations of CO2 at 1 atmosphere and by O2 at 3.0 atmospheres. *J Appl Physiol* 5: 803–813, 1953. doi:10.1152/jappl.1953.5.12.803.

36. **Kuenzel A**, **Marshall B**, **Verges S**, **Anholm JD.** Positional changes in arterial oxygen saturation and end-tidal carbon dioxide at high altitude: Medex 2015. *High Alt Med Biol* 21: 144–151, 2020. doi:10.1089/ham.2019.0066.
37. **Mack GW**, **Lin YC.** Isoproterenol infusion promotes nitrogen washout in rats under normobaric conditions. *J Appl Physiol Respir Environ Exerc Physiol* 57: 1306–1311, 1984. doi:10.1152/jappl.1984.57.5.1306.
38. **Aukland K**, **Berliner RW.** Measurement of Local Blood Flow with Hydrogen Gas. *Circ Res* 14: 164–187, 1964. doi:10.1161/01.res.14.2.164.
39. **Leonard EF**, **Jørgensen SB.** The analysis of convection and diffusion in capillary beds. *Annu Rev Biophys Bioeng* 3: 293–339, 1974. doi:10.1146/annurev.bb.03.060174.001453.
40. **Campbell JA**, **Hill L.** Studies in saturation of the tissues with gaseous nitrogen.—I. Rate of saturation of goat's bone marrow in vivo with nitrogen during exposure to increased atmospheric pressure. *Exp Physiol* 23: 197–210, 1933. doi:10.1113/expphysiol.1933.sp000594.
41. **Doolette DJ**, **Upton RN**, **Grant C.** Altering blood flow does not reveal differences between nitrogen and helium kinetics in brain or in skeletal miracle in sheep. *J Appl Physiol (1985)* 118: 586–594, 2015. doi:10.1152/japplphysiol.00944.2014.
42. **Lesser GT**, **Deutsch S.** Measurement of adipose tissue blood flow and perfusion in man by uptake of 85Kr. *J Appl Physiol* 23: 621–630, 1967. doi:10.1152/jappl.1967.23.5.621.
43. **Evans AL**, **Busuttil A**, **Gillespie FC**, **Unsworth J.** The rate of clearance of xenon from rat liver sections in vitro and its significance in relation to intracellular diffusion rates. *Phys Med Biol* 19: 303–316, 1974. doi:10.1088/0031-9155/19/3/002.
44. **Hennessy TR.** The interaction of diffusion and perfusion in homogeneous tissue. *Bull Math Biol*, 36: 505–526, 1974. doi:10.1007/BF02463263.
45. **Ohta Y**, **Song SH**, **Groom AC**, **Farhi LE.** Is inert gas washout from the tissues limited by diffusion? *J Appl Physiol Respir Environ Exerc Physiol* 45: 903–907, 1978. doi:10.1152/jappl.1978.45.6.903.
46. **Doolette DJ**, **Upton RN**, **Grant C.** Perfusion–diffusion compartmental models describe cerebral helium kinetics at high and low cerebral blood flows in sheep. *J Physiol* 563: 529–539, 2005. doi:10.1113/jphysiol.2004.077842.
47. **Murphy FG**, **Hada EA**, **Doolette DJ**, **Howle LE.** Probabilistic pharmacokinetic models of decompression sickness in humans, part 1: Coupled perfusion-limited compartments. *Comput Biol Med* 86: 55–64, 2017. doi:10.1016/j.compbiomed.2017.04.014.
48. **Murphy FG**, **Hada EA**, **Doolette DJ**, **Howle LE.** Probabilistic pharmacokinetic models of decompression sickness in humans: Part 2, coupled perfusion-diffusion models. *Comput Biol Med* 92: 90–97, 2018. doi:10.1016/j.compbiomed.2017.11.011.
49. **Europäische Gemeinschaft für Kohle und Stahl, European Respiratory Society, European Respiratory Society.** Quanjer PH, editors**.** *Lung volumes and forced ventillatory flows. Standardized lung function testing: report; official statement of the European Respiratory Society*. Copenhagen: Munksgaard, 1993.
50. **Hawkins JA**, **Shilling CW.** Nitrogen solubility in blood at increased air pressures. *J Biol Chem* 113: 273–278, 1936. doi:10.1016/S0021-9258(18)74912-0.
51. **Bove AA.** Risk of decompression sickness with patent foramen ovale. *Undersea Hyperb Med* 25: 175–178, 1998.
52. **Germonpré P.** Patent foramen ovale and diving. *Cardiol Clin* 23: 97–104, 2005. doi:10.1016/j.ccl.2004.10.005.
53. **Madden D**, **Ljubkovic M**, **Dujic Z.** Intrapulmonary shunt and SCUBA diving: another risk factor? *Echocardiography* 32 *Suppl 3*: S205–S210, 2015. doi:10.1111/echo.12815.